Proceedings of 10th International Conference on Precision, Meso, Micro and Nano Engineering (COPEN 10)
December 07 – 09, 2017, Indian Institute of Technology Madras, Chennai – 600 036 INDIA

Electrochemical micro-texturing using microelectrodes array fabricated through wire-EDM on SS-304: experiments and simulation

Divyansh S. Patel[1]*, Mahesh Thalkar[1], V. K. Jain[2], J. Ramkumar[1]
[1] Department of Mechanical Engineering, Indian Institute of Technology Kanpur, Kanpur -208016, India
[2] Department of Mechanical Engineering, M. A. N. I. T. Bhopal, Bhopal - 462003, INDIA

Abstract

Texturing through electrochemical sinking process requires a sophisticated microelectrode tool design and fabrication methodology. Wire-electric discharge machining (Wire-EDM) is one of the promising techniques of manufacturing for large area texturing, production of micro-pillars (microelectrode) array is a challenging problem and has no previous study reported. The paper outlines a novel methodology of production of microelectrodes array through machining micro-channels array using Wire-EDM. Micro wire of 180 µm is used for the production of arrays of microchannels and square microelectrodes of 150 µm are achieved through machining channels in two normal directions on a copper tool. Produced microelectrodes are spaced 200 µm apart and, height of microelectrode is 200 µm. Experimental geometrical parameters of multiple microelectrode array tool are used for conducting simulation of EC sinking operation for microtexturing on SS304 workpiece. Further, validation of results of EC texturing is done using EC micro-texturing through wire-EDMed microelectrodes array tool. Finally, arrays of square micro-dimples (of width ≈ 200 µm) are machined and compared with simulated results.

Keywords: Micro-pillars, micro-channels, micro-dimples, Wire EDM, EC texturing, voltage, current.

1. INTRODUCTION

Hydrophobicity, surface free energy, interfacial free energy and surface topology are the key parameters which influence the interface of an implant surface with the atmosphere inside a human body. Cell attachment and human fibroblast spreading can be regulated by contact angle of interacting substance to surface of the implant [1,2]. In the field of tribology and machining, researchers are mimicking natural surfaces for reducing the friction, wear and enhancing tribological properties [3,4]. From last few decades, it has become a trend to replicate the natural surfaces for example, lotus leave, shark-riblet structures etc. so as to achieve their vibrant multifunctional characteristics. It is found microscopically that super-hydrophobicity of a lotus surface exists for the reason that the microdroplet contacts at multiple locations of the hierarchical structure. There is no direct contact between the liquid and solid due to existence of air (gas), which results a composite mode of contact. Gecko feet and rose petals inspired surfaces are being produced for achieving high-adhesion super-hydrophobic surface [5]. A number of functions such as water repellency, self-cleaning, and defense against pathogens of these bioinspired surfaces are being replicated on metals and alloys to protect aero-foils and aircraft engines against the accumulation of ice during high altitude fly as well as, to make more weather proof infrastructures. The area of applications of hydrophobicity is quite wide, including power transmission lines, pipes of air conditioners and refrigerators drag reduction, radar or tele- communication antennas, weather proof infrastructures etc. There are recent studies for producing textures on metals using electrochemical machining because of its advantages of machining any hard-to-machine metals at micro-/nanometer level without any heat affected zone [6–9].

Micro texturing

Surface texturing is the process of generating a specific pattern of multiple micro features on the workpiece surface in order to change its functional properties. Surface texturing with micro features on multiple scales can be produced in micro/ nanometer range, which enables many new applications of the engineered surfaces. The specific surface texture can be used to influence functional properties, e.g., wetting, tribological characteristics (friction and wear), optical properties etc. Generally, these surfaces are referred as functional surfaces. The term “texturing” defines the engineered surfaces that contain multiple engineered features (micro-holes, micro-asperities, micro-dimples, micro-/nano-hairs, micro-patterns at multiple levels etc.) of same geometrical parameters, which are purposely manufactured in order to enhance the functionality of the surface in the given environment.

This work presents a comprehensive study of micro-texturing through electrochemical sinking using micro-electrodes array machined through Wire-EDM. The work is theoretically supported by 3-D modelling of EC texturing of micro-dimples using COMSOL. The numerical modelling of the process reveals prediction of anode shape deformation by estimating the current density and potential at zone of machining. There are several studies related to modelling of electrochemical micromachining, glimpse of some are discussed here. Liua et al. [10] proposed analytical solution for tool shape correction or to avoid overcut in machining of turbine blade by electrochemical machining process. Current density distribution on workpiece surface is simulated using COMSOL and shape evolution of the turbine blade tip is reported. Qian et al. [11] presented a modified through mask electrochemical micromachining (TMEMM), in which the insulation layer was directly attached to the cathode, was developed to produce micro-dimples on the hard chrome-coated surface. Laplace equation is solved with initial and boundary conditions in FEM to predict electric field and current density distribution over workpiece surface. Klocke et al. [12] demonstrated a multi-physical approach for modeling the ECM material removal process by coupling all relevant conservation equations, model validated on compressor blades. COMSOL Multiphysics has been used for modeling and simulation the of the process. Chen et al. [13] presented Multiphysics simulation of electrochemical machining process by using pulses. A simplified algorithm based on the quasi steady state shortcut (QSSSC) is introduced to reduce the

ISBN: 978-93-80689-28-9

processing time in simulation of PECM process. COMSOL Multiphysics 5.2 used for simulation. There are very few theoretical studies simulating mask-less electrochemical machining, and a clear research gap (due to no work reported) for 2-D/3-D numerical modeling for EC surface texturing.

2. NUMERICAL SIMULATION EC TEXTURING

Geometrical and physical parameters of the machined textures are simulated using a sophisticated 3-D numerical modelling tool. Current density is the key parameter which leads to formation and physical parameters of the crater on the machined surface. Analysis of the current density distribution on domain of interest (i.e. IEG) results in estimation of the profile and dimensions of the micro-dimples array produced through micro-electrode array tool. The 3-D geometry framed in COMSOL is shown in Fig. 1(a). The formulations begin with discretising the domain of interest and meshing with free triangular mesh elements. Laplace's equation is solved in the domain using FEM with the necessary boundary conditions to obtain the potential at each point of the anode.

$$\nabla^2 v=0 \qquad (1)$$

Where, ∇ is Laplace operator and v is potential field in electrolyte domain or nearby to electrode surface. In cartesian co-ordinate Laplace equation defines conservation of potential field in electrolytic domain. Laplace equation is solved to give potential v at any point in electrolyte domain with necessary boundary conditions.

$$J_n = - \sigma \cdot \nabla v \qquad (2)$$

Where, J_n is the current density, it can be found by potential field solved by Laplace equation *(1)*.

$$V_n=A \cdot J_n / z \cdot F \cdot \rho \qquad (3)$$

Where, $k = (A / z \cdot F \cdot \rho)$ constant for Anode material. All the parameters other than J_n for a particular material can be combined together into a constant denoted by k. Faraday's equation is used to give anode recession rate V_n in in the normal direction. A being the atomic weight, z is valency, F is Faraday's Constant equal to 96500 *C/mol*, ρ be the density of work piece material and J_n is current density in the normal direction obtained from Eq. *(2)*. We know that most commercial materials in use are alloys. Thus, the expression of V_n modified for alloy material is

$$V_n = -\frac{1}{F}\left(\sum_i \frac{(W_i/100)A_i}{\rho_i \cdot z_i}\right) \cdot J_n \qquad (5)$$

Where, i is the summation index denoting number of elements in the alloy and W_i is the weight percentage of a particular element in the alloy (or overall mixture). COMSOL Multiphysics software is used to simulate the development of the desired texture on the work piece. A 3D model was formulated using the electric current sub-module under its AC/DC module, deformed mesh sub-module under the mathematics module and Turbulent flow sub- module under fluid flow module to analyze flow pattern around the tool electrode and in machining areas.

2.1 Mathematical formulation

Simple geometric model being used with array of 16 tool electrode of Copper (Cu). Electrolyte with conductivity of 10 S/m is used. Inter electrode gap set to 50 µm. Simulation executed with fine triangular mesh. Electric current, deformed geometry and turbulent flow these three physics are solved simultaneously in this simulation process. Electric current physics is applied to all three domains.

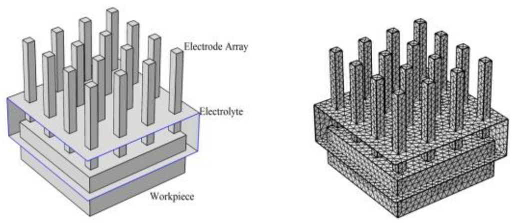

Fig. 1. (a) 3D Geometry Showing Array of the tool, Workpiece and Electrolyte with two side open (b) Fine triangular mesh on tool-electrodes, electrolyte and the workpiece

Local charge density varies with divergence of current density,

$$\nabla \cdot J=Q_j \qquad (6)$$

With the specific electric conductance σ, the electric displacement field ε0εrE and the external vector of current density J_e the vector of current density results to

$$J = (\sigma+\varepsilon_0\varepsilon_r \cdot \partial/\partial t)E + J_e \qquad (7)$$

Equation *(7)* is outcome of Ohm's equation given by equation *(2)*. E in above equation is the electrical field is defined by the negative gradient of electric voltage

$$E=-\nabla v \qquad (8)$$

All outer boundaries and side boundaries of tool electrodes are electrically insulated with $n \cdot J=0$. Ground potential is applied at bottom face of tool electrode with $v = 0$. Electric Potential with $v = 10\ V$ is applied at anode surface. Deformed Geometry physics is applied to analyze deformation of workpiece. Boundaries oriented in x y and z direction are prescribed with velocity $V_x=0$, $V_y=0$, $V_z=0$ respectively. Top surface of workpiece where ablation take place is prescribed with normal ablation velocity $V_n= -k \cdot (ec.nJ)$, Where, V_n is ablation velocity of workpiece in normal direction. *ec.nJ* is normal current density obtained in electric current module. The value of the constant k depends on the composition of the material of the workpiece. In the present case, SS-304 (stainless steel) is considered as a workpiece. The value of k from composition along with the density and electrochemical equivalence arises to $3.4 \times 10^{-11}\ m^3/A \cdot s$. Flow field in process can be completely described by Navier-Stokes equation. Turbulent flow physics applied to electrolyte domain, Navier- Stokes equation used to observe velocity at different points of machining area,

$$\rho(u \cdot \nabla)u = \nabla \cdot [-\rho I+\mu(\nabla u + (\nabla u)^T) - 2/3 \cdot \mu(\nabla \cdot u)I]+F \qquad (9)$$

Here ρ denotes density of electrolyte u be the velocity vector, F being external force. Along with above equation, equation of continuity for charge conservation is solved for Newtonian flow

$$\nabla\cdot(\rho u) = 0 \tag{10}$$

Inlet velocity is given to inlet face with boundary conditions $u=-U_0\cdot n$. Exit Boundary condition,

$$[-\rho I+\mu(\nabla u + (\nabla u)^T) - 2/3\cdot\mu(\nabla\cdot u)I]n = P_0 n \tag{11}$$

and $u.t = 0$. All internal wall solved with no slip boundary condition with $u=0$ at boundary interface.

3. Micro-electrodes array fabrication

Wire-ED Texturing

produce micro-channels array in two perpendicular directions. Micro-electrodes array of ≈ 150 µm are produced at the distance of 200 µm. Figure 4 shows the dimensioned microscopic and 3-D profile images of micro-electrodes array produced.

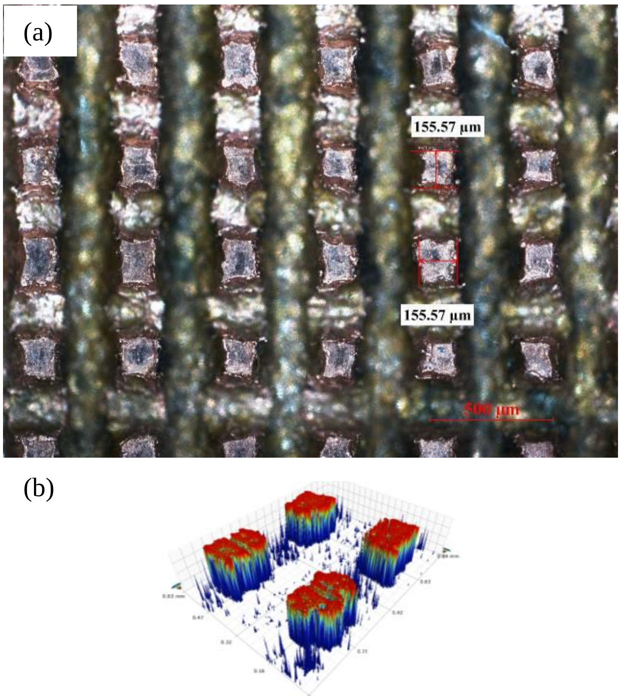

Fig. 2. (a) Micro-electrodes array machined on Cu through Wire-EDM, (b) 3-D profilometry image of micro-electrodes

Figure 2(a) shows micro-electrodes of square cross section, having width of 150±10 µm. Figure 2(b) 3-D profilometry image of textured surface with Wire-EDM, which reveals depth and pitch of the micro-electrodes. The depth of micro-pillars is 100±5 µm and the distance between the two pillars is ≈ 200 µm.

3. Results and discussion

3.1 Simulation results

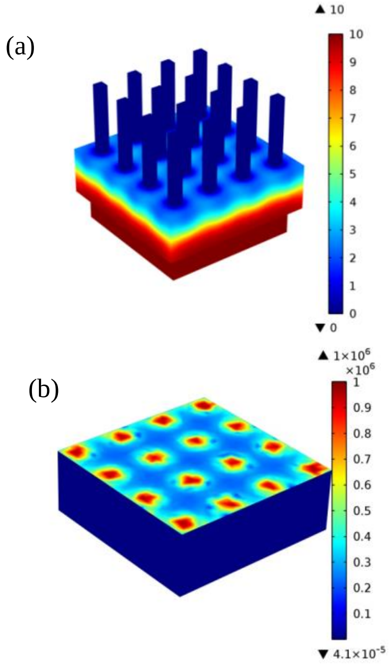

Fig. 3. (a) Potential drop across the electrodes, electrolyte and the workpiece (in V), (b) Current density distribution on electrodes (anode) (in A/m^2)

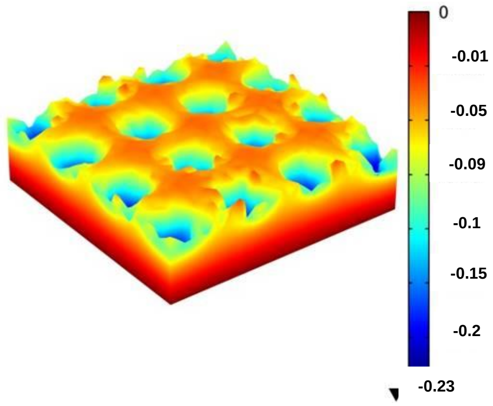

Fig. 4. Simulated 3-D profile of micro-dimples array on SS304 (dimensions in m)

Experiment is simulated by keeping constant machining time of 10 s and conductivity of 10S/m. Fig. 3(a) shows the potential difference at different zones of electrochemical texturing system. When the current density is simulated on the anode, it is found that the nature of current density is a bell-shaped curve (when plotted in 2-D). Current density is the maximum at the center of the single micro-electrode as the tool is insulated from all the side. Fig. 3(b) shows maximum current density of 1×10^6 A/m^2 at the location of micro-electrodes at the anode when applied voltage is 10 V. Fig. 4 shows 3-D simulated profile of the textured surface of SS304 with micro-dimples. Since current density at the anode cathode interface is proportional to MRR, Dimple of ≈ 220 µm depth and 0.28 mm diameter is observed on anode surface. 3-D numerical model of electrochemical texturing provides significant knowledge of the final deformed surface. By varying the input parameters, the experiments are performed repeatedly and the range process parameters are selected for experimental investigation of electrochemical texturing.

3.2 Electrochemical Texturing

Electrochemical sinking operation is carried out using the tool of copper with micro-electrodes array. The specific values of input process parameters are selected through multiple simulation at different ranges of parameters. The electrolyte used is 1M $NaNO_3$, input voltage of 10 V, inter-electrode gap of 50 µm. Figure 5(a) shows optical microscopy image of surface textures machined on SS304. The maximum depth of the micro-dimples is 100±10 µm, whereas width of the square micro-dimples obtained is 200±10 µm. Magnified view of a micro-dimple is on the left is showing the profile and marks of stray current machining. Figure 5(b) shows the 3-D image of micro-dimples array (with dimensions) produced through EC texturing.

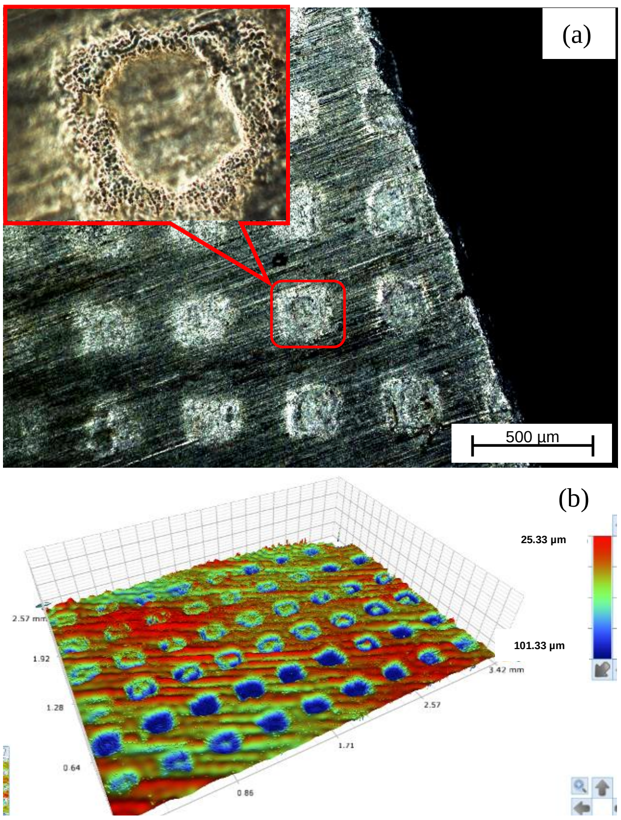

Fig. 5. (a) Square micro-dimples array and magnified view of a micro-dimple produced through EC texturing on SS304, (b) 3-D optical profilometry image of micro-dimples array

A novel 3-D numerical modelling for electrochemical texturing for producing micro-dimples array on a stainless-steel surface is introduced for the first time, using software COMSOL 4.3a. Estimation of current density and potential between the inter-electrode-gap helps in predicting the anode shape deformation. No. of experiments are performed to select the specific value of the major input parameters. A method of microelectrode array fabrication has been proposed using Wire-EDM. Micro-pillars are obtained on a flat surface of Cu with height ranging from 100±5 µm and width 150±10 µm. EC sinking with this multi-electrode tool array leads to the production of square micro-dimples of 200±10 µm spaced at 200±10 µm distance. Comparison of theoretical and experimental results validates the study closely.

REFERENCES

[1] Ponsonnet L, Reybier K, Jaffrezic N, Comte V, Lagneau C, Lissac M, Relationship between surface properties (roughness, wettability) of titanium and titanium alloys and cell behaviour. Mater Sci Eng C, **23** (2003) 551–60.

[2] Kubiak KJ, Wilson MCT, Mathia TG, Carval P. Wettability versus roughness of engineering surfaces, Wear, **271** (2011) 523–528.

[3] Niketh S, Samuel GL, Surface texturing for tribology enhancement and its application on drill tool for the sustainable machining of titanium alloy, J Clean Prod, 2017, DOI: 10.1016/j.jclepro.2017.08.178.

[4] Walker JC, Kamps TJ, Lam JW, Mitchell-smith J, Clare AT, Tribological behavior of an electrochemical jet machined textured Al-Si automotive cylinder liner material. Wear, **376–377** (2017) 1611–1621.

[5] Liu M, Zheng Y, Zhai JIN, Jiang LEI, Bioinspired Super-antiwetting Interfaces with Special Liquid-Solid Adhesion, **43** (2010) 368-377.

[6] Yang X, Liu X, Lu Y, Zhou S, Gao M, Song J, et al. Controlling the Adhesion of Superhydrophobic Surfaces Using Electrolyte Jet Machining Techniques. Sci Rep. Nature Publishing Group; **6** (2016) 1-9. DOI: 10.1038/srep23985.

[7] Patel DS, Jain VK, Shrivastava A, Ramkumar J, Electrochemical micro texturing on flat and curved surfaces: simulation and experiments. Int J AdvManuf Technol, (2016). DOI:10.1007/s00170-016-9700-3.

[8] Patel D, Jain VK, Ramkumar J, Micro texturing on metallic surfaces: State of the art. Proc IMechE Part B: J Engineering Manufacture, (2016), DOI: 10.1177/0954405416661583.

[9] Silva LRR, Costa HL, Tribological behavior of gray cast iron textured by maskless electrochemical texturing, Wear, **376–377** (2017)1601–1610.

[10] Liua WD, Aoa SS, Lia Y, Zhaoa CF, Luoa Z, Lic Q, Luoda T, Elimination of the over cut from a repaired turbine blade tip post-machined by electrochemical machining, J of Mate Pro Technol, **231** (2016) 27–37.

[11] Qian S, Zhu D, Qu N, Li H, Yan D, Generating micro-dimples array on the hard chrome-coated surface by modified through mask electrochemical micromachining, Int J Adv Manuf Technol, **47** (2010) 1121–112.

[12] Klockea F, Zeisa M, Harsta S, Klinka A, Veselovaca A, Baumgärtnerb A, Modeling and Simulation of the Electrochemical Machining (ECM) Material Removal Process for the Manufacture of Aero Engine Components, Procedia CIRP, **8** (2013) 265–270.

[13] Chen Y, Fang M, Jiang L, Multiphysics simulation of the material removal process in pulse electrochemical machining (PECM), Int J Adv Manuf Technol, **91** (2017) 2425-2464.